EJECTA PROPERTIES OF ZI WEI CRATER AS REVEALED BY CHANG'E-3 LUNAR PENETRATING RADAR. Wenzhe Fa, Institute of Remote Sensing and Geographical Information System, Peking University, Beijing 100871, China (wzfa@pku.edu.cn).

Introduction: During an impact cratering event, target materials at depth are fragmentized, excavated, and ejected, and then fall back onto the surface, forming an ejecta blanket surrounding the crater. Eejecta properties such as thickness, particle size distribution, and porosity are critical for understanding the impact cratering mechanism and postimpact surface modification process.

On December 14, 2013, China's Chang'E-3 (CE-3) spacecraft successfully landed on the east rim of a 500 m crater (named as Zi Wei crater by IAU; Fig. 1 in [1-3]). The depth of the crater is ~50 m, corresponding to a depth/diameter ratio of 0.1. Images from CE-3 panoramic cameras show abundant rocks within the crater rim, whereas almost no meter-scale rocks occur outside the rim [3]. According to the morphological prominence [4], the age of this crater is estimated as ~100 Myr [3]. The lunar penetrating radar (LPR) aboard the Yutu rover can penetrate more than 10 m beneath the surface [5], providing a glimpse for ejecta properties of this young fresh crater. Here I report ejecta thickness, rocks distribution, dielectric permittivity, and porosity of Zi Wei crater as inferred from the CE-3 LPR observations.

Lunar Penetrating Radar Data Processing: CE-3 LPR is an ultra wide band ground penetrating radar (GPR) operating at 60 and 500 MHz [5]. The nominal penetration depth of the LPR is ~10 wavelengths if a dielectric permittivity of 3+i0.03 is used based on regolith composition. During its two-month lifetime, the LPR worked for ~8.3 hours and obtained a subsurface GPR cross-section with a lateral distance of ~110 m. In this study, only observations from high frequency channel are used. The raw data were processed through repetitive observation removal, horizontal band removal, band-pass filtering, compensation of geometrical spreading and dielectric attenuation, and range migration [3]. The processed LPR data are displayed in B-scan format as a function of horizontal distance and apparent depth (Fig. 1).

Ejecta Properties of Zi Wei Crater: The most prominent feature in Fig. 1 is a region (above the cyan line) with bright radar echoes. This region contains numerous, chaotic, irregular layers and hyperbolic curves (red dots). The layering may result from irregular interface geometry or discontinuities of the dielectric properties. In GPR images, hyperbolic curves are usually produced by discrete scatterers, and here are most probably rocks. This region should be the continuous ejecta blanket.

To model the trace of the hyperbola, a homogeneous ejecta layer with buried rocks is assumed. As the LPR moves over a buried rock along the survey line, the direct-line distance between radar antenna and the subsurface rock decreases until the LPR is over the rock, and then increases as the LPR moves away. As a result, the trace of a buried rock appears as a hyperbola in GPR image (Fig. 2). The geometry of the hyperbola can be indicated by its eccentricity, which can be obtained by the trace of the curve. Simulation of radar wave propagation based on geometry optics shows that eccentricity of the hyperbola depends mainly on real part of the dielectric permittivity and depth of the buried rock. This can be used to estimate real part of the dielectric permittivity.

Thickness. The base (the cyan line) of the ejecta is identified visually based on relative strength and the texture of the LPR image. With a dielectric permittivity of 3+ i0.03 based on regolith composition, ejecta thickness is estimated to be from ~2.5 m to ~6 m, with a mean value of 5.3 m. This is consistent with the predicted ejecta thickness of 4 m at a location that is 50 m from the rim of a 500 m crater using the model in McGetchin et al. [6], but is much smaller than the value of 8.3 m based on the model in Arvidson et al. [7].

Rock number. Here, a rock is identified as the vertex of a hyperbola. Given to the large dynamic range of the radar echo, the contrast and brightness of local LPR image were adjusted in order to identify a rock confidently. In Fig. 1, the red dots represent the identified rocks. The rock number at a given depth along the survey line is counted, and then normalized by the length of the survey line. Finally, histogram of rock number as a function of depth is obtained. Results show that number of fragments increases with depth, reaching to a maximum value at a depth of ~1.8 m, and then decreases with depth. This probably represents a balance between initial deposition of ejecta and later turnover of regolith by micrometeorite bombardments.

Real part of the dielectric permittivity. The relation between the eccentricity of a hyperbola and real part (ε) of the dielectric permittivity can be obtained from simulation based on geometrical optics, which can be used for dielectric permittivity estimation. In total, 57 typical hyperbolas in Fig. 1 were identified, and then their eccentricities were obtained by fitting the curve to a hyperbola. The estimated real part of the dielectric

permittivity varies from 1.1 to 6.1, with a mean value of 3.2. This is consistent with the model predicted relative permittivity of 3.0+i0.03 based on the FeO and TiO_2 abundances of 19.5 wt.% and 5.2 wt.% and a typical porosity of 45% [8].

Bulk density and porosity. Measurements of the dielectric permittivity of Apollo regolith samples show that real part of the dielectric permittivity depends mainly on bulk density (ρ) as $\varepsilon = 1.919^{\rho}$[8]. Using this relation, mean bulk density of the regolith as a function of depth can be inverted (Fig. 3). The inversion results show that bulk density increases with depth, and that there is no obvious trend in lateral variation of the bulk density. The bulk density can be modeled as $\rho(z) = \rho_d - (\rho_d - \rho_s)e^{-z/H}$, where $\rho_s = 0.86$ g/cm^3 is the surface density, $\rho_d = 2.27$ g/cm^3 is subsurface steady-state density, and $H = 1.05$ m is the *e*-folding depth scale. Based on the FeO and TiO_2 abundances, zero-porosity density of the regolith at the landing site is 3.32 g/cm^3. Using the estimated bulk density, porosity of the crater ejecta is about 71.4% at the surface and 31.7% at a depth of 5 m.

Conclusions: In this study, CE-3 high-frequency LPR observations are used to investigated thickness, real part of the dielectric permittivity, rock abundance, bulk density, and porosity of the ejecta of the Zi Wei crater. Results show that rock number increases with depth to ~1.8 m and then decreases with depth, and that real part of the dielectric permittivity and bulk density increase with depth. All these can provide important information on the formation and evolution of the ejecta of the Zi Wei crater.

Acknowledgements: This work was supported by the National Natural Science Foundation of China (No. 11573005)

References: [1] Xiao L. et al. (2015) *Science, 347,* 1226–1229. [2] Ling Z. et al. (2015) *Nature Communications, 6,* 8880. [3] Fa W. et al. (2015) *GRL, 42,* doe: 10.1002/2015GL066537. [4] Basilevsky, A. T. (1976) *LPSC, 7,* 1005–1020. [5] Fang G. et al. (2014) *RAA, 14*, 1607–1622. [6] McGetchin T. et al. (1973) *EPSL*, *20*, 226–236. [7] Arvidson R. et al. (1975) *The Moon*, *13*, 67–79. [8] Heiken G. H. et. al. (1991) New York: Cambridge Univ. Press. [9] Fa W., and M. Wieczorek (2012), *Icarus*, *218*, 771–787.

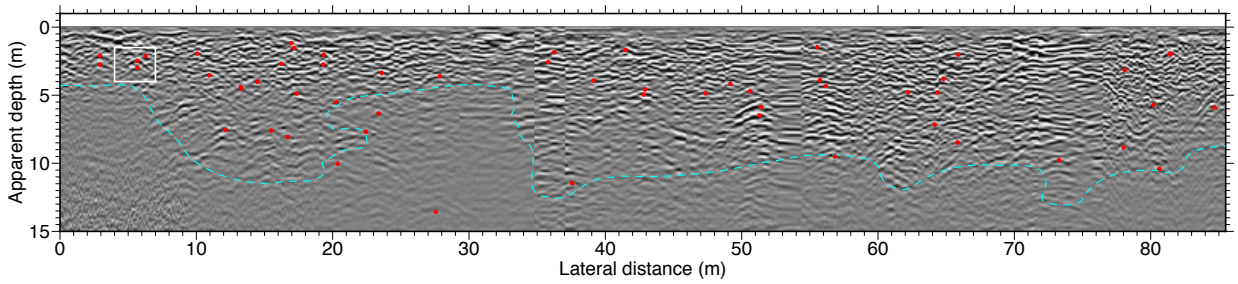

Figure 1. LPR image at 500 MHz along the Yutu survey line. The cyan line shows the base of the ejecta layer, and the dots indicate the vertexes of identified hyperbolic curves.

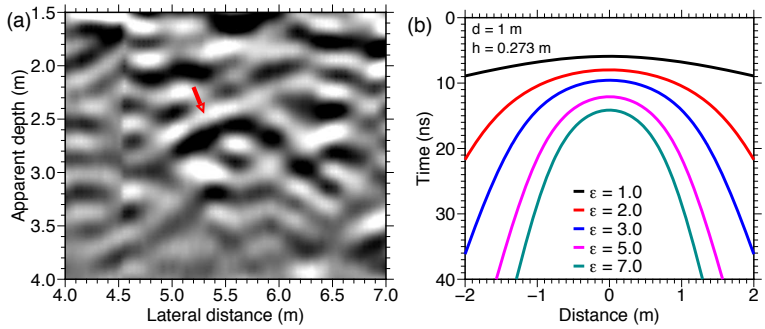

Figure 2. (a) a typical hyperbola in LPR image. (b) The traces of GPR echoes from a buried rock with different dielectric permittivity of the lunar subsurface material. The depth of buried rock is 1.5 m, and the height of the antenna is 0.273 m.

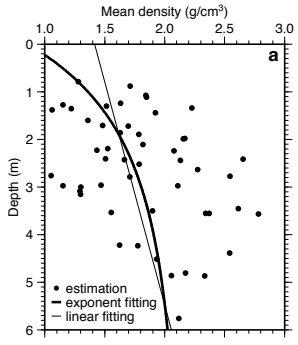

Figure 3. Mean bulk density as a function of depth, the dots are estimations from CE-3 LPR observations, and the thick and thin lines are best fits of the estimations using exponent and linear functions.